Bioorganic & Medicinal Chemistry Letters 23 (2013) 5014–5021

Contents lists available at SciVerse ScienceDirect

Bioorganic & Medicinal Chemistry Letters

journal homepage: www.elsevier.com/locate/bmcl

2-Amino-[1,2,4]triazolo[1,5-*a*]pyridines as JAK2 inhibitors

Michael Siu [a,*], Richard Pastor [a], Wendy Liu [a], Kathy Barrett [a], Megan Berry [a], Wade S. Blair [a], Christine Chang [a], Jacob Z. Chen [a], Charles Eigenbrot [a], Nico Ghilardi [a], Paul Gibbons [a], Haiying He [b], Christopher A. Hurley [c], Jane R. Kenny [a], S. Cyrus Khojasteh [a], Hoa Le [a], Leslie Lee [a], Joseph P. Lyssikatos [a], Steve Magnuson [a], Rebecca Pulk [a], Vickie Tsui [a], Mark Ultsch [a], Yisong Xiao [b], Bing-yan Zhu [a], Deepak Sampath [a]

[a] *Genentech, Inc., 1 DNA Way, South San Francisco, CA 94080, United States*
[b] *WuXi AppTec Co., Ltd., 288 Fute Zhong Road, Waigaoqiao Free Trade Zone, Shanghai 200131, PR China*
[c] *Argenta, 8/9 Spire Green Centre, Flex Meadow, Harlow, Essex CM19 5TR, United Kingdom*

ARTICLE INFO

Article history:
Received 8 March 2013
Revised 28 May 2013
Accepted 3 June 2013
Available online 15 June 2013

Keywords:
JAK2
Janus kinase
Triazolopyridine

ABSTRACT

The advancement of a series of ligand efficient 2-amino-[1,2,4]triazolo[1,5-*a*]pyridines, initially identified from high-throughput screening, to a JAK2 inhibitor with pharmacodynamic activity in a mouse xenograft model is disclosed.

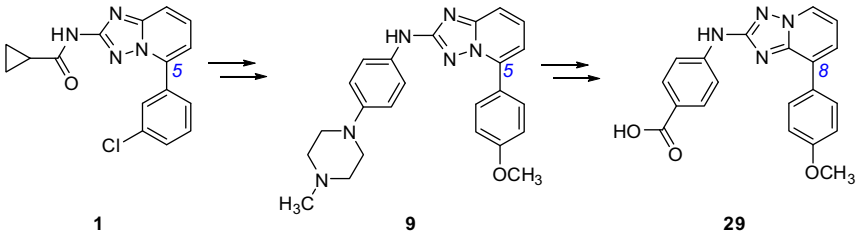

1
JAK2 K_i = 0.0597 uM
LE = 0.45

9
JAK2 K_i = 0.0006 uM
LE = 0.41

29
JAK2 K_i = 0.0017 uM
LE = 0.45

JAK2 (Janus kinase 2) is a member of a family of non-receptor cytoplasmic tyrosine kinases which include JAK1, JAK3, and TYK2.[1] This family of kinases share similar structural motifs, and all have a JH1 kinase domain at the C terminus with an adjacent JH2 pseudokinase domain. The JAK/TYK kinases are activated upon cytokine to cytokine receptor binding. Transduction of the cytokine signal occurs by phosphorylation of STAT (signal transducers and activators of transcription) proteins that proceed to upregulate their respective target genes. Mutation of JAK2 at codon 617 from valine to phenylalanine (V617F) in the pseudokinase domain is prevalent in myeloproliferative diseases.[2] This particular mutation leads to kinase activity without cytokine activation in hematopoeitic cells. In chronic myeloproliferative diseases, the activating JAK2 V617F mutation is found in >95% of patients with polycythemia vera (characterized by overproduction of red blood cells), in ~50% of patients with essential thrombocythemia (characterized by overproduction of platelets), and in ~50% of patients with myelofibrosis (characterized by fibrosis of the bone marrow).[3] Accordingly, the inhibition of JAK2 presents an opportunity for targeted therapy for these myeloproliferative diseases.

A variety of JAK inhibitors have been reported in the literature[4] and have entered clinical trials[5] with the most advanced being tofacitinib (JAK1/JAK3 inhibitor)[6] and ruxolitinib (JAK1/JAK2 inhibitor).[7] Herein, we disclose our initial efforts toward JAK2 inhibitors from chemical matter discovered by high-throughput screening with the goal of generating a compound with greater than 10-fold biochemical selectivity for JAK2 over JAK1, JAK3, and TYK2.

In order to identify novel small molecule JAK2 inhibitors, our internal collection of small molecules was screened against the

* Corresponding author. Tel.: +1 650 467 7764; fax: +1 650 467 8922.
E-mail address: siu.michael@gene.com (M. Siu).

0960-894X/$ - see front matter © 2013 Elsevier Ltd. All rights reserved.
http://dx.doi.org/10.1016/j.bmcl.2013.06.008

kinase domain of JAK2. For the primary screen, percent inhibition was measured at a concentration of 5 μM. For a subset of compounds which showed >50% inhibition, half-maximal inhibitory concentrations (IC_{50}) were determined. Based on these activity measurements, the 5-substituted 2-amino-[1,2,4]triazolo[1,5-*a*]pyridine **1**[8] was one of the chemotypes selected for optimization that had high ligand efficiency (Table 1, LE = 0.45).[9] This chemotype was potent against JAK2 but not selective against JAK1 and TYK2 (Table 1). For initial SAR development, both the cyclopropyl and chlorophenyl positions were explored via parallel synthesis (representative examples shown in Table 1). An approximate 7.5-fold improvement in JAK2 biochemical potency was achieved by introduction of appropriate lipophilicity on the aryl ring while maintaining high ligand efficiency (*iso*-propylphenyl analog **4**, Table 1); however, close-in replacements of the cyclopropanecarboxamide (propionamide **7** and benzamide **8**) did not maintain the necessary binding affinity (Table 1). Moreover, sulfonamides such as methylsulfonamide and cyclopropylsulfonamide at the R1 position were not tolerated (data not shown).

To further improve on our initial analogs, structure-based design efforts were also undertaken. As attempts to obtain a crystal structure of triazolopyridine **1** in the active site of JAK2 were unsuccessful, a docking protocol using the JAK2 crystal structure of TG101209[10,11] was developed to generate a model of the JAK2-**1** complex. The protein was prepared using the default settings in the Protein Preparation Workflow in Maestro[12] and **1** was docked using Glide[13] after preparation with LigPrep using the default settings (LigPrep, version 2.4, Schrödinger, LLC, New York, NY, 2010.)

This comparison of the triazolopyridine **1** to TG101209 (Fig. 1) suggested that the cyclopropanecarboxamide could be replaced with a phenylpiperazine moiety in order to improve van der Waals interactions in the active site. We synthesized a series of phenylpiperazine containing analogs shown in Table 2. Methoxyphenyl and methylsulfonylphenyl analogs were initially examined on the scaffold to balance the additional lipophilicity of the phenylpiperazine group. In general, these substitutions led to significant inhibitory activity of JAK2 in the biochemical assay. From this initial examination, *meta*-substitution or large *para*-substitution on the 5-aryl ring improved JAK2 selectivity over JAK1. Moreover, these compounds were potent in our cellular assay—inhibition of phosphorylation of STAT5 in SET-2 cells with triazolopyridine **9** being the most potent.

Triazolopyridine **9** is synthesized as shown in Scheme 1. Treatment of 2-amino-6-bromopyridine with ethyl isothiocyanatoformate provides thiourea **14** which cyclizes to the triazolopyridine core **15** upon treatment with hydroxylamine hydrochloride. Palladium catalyzed cross coupling of bromide **15** with 4-methoxyphenylboronic acid provides amine **16**. Diazotization of amine **16** with sodium nitrite and in situ trapping with iodide give iodide **17**. Lastly, palladium catalyzed amination of iodide **17** with 4-(4-methylpiperazin-1-yl)aniline affords triazolopyridine **9**.

Table 1

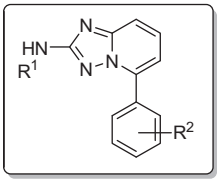

Ex	R^1	R^2	JAK2 K_i (μM)	JAK1 Sel Indx[a]	JAK3 Sel Indx[b]	TYK2 Sel Indx[c]	*C*log*P*[d]	LE
1		3-Cl	0.0597	0.7×	15×	1.1×	3.4	0.45
2		4-Cl	0.059	0.3×	8.4×	1.6×	3.4	0.45
3	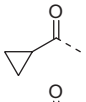	3-CF_3	0.0826	0.44×	18.8×	1.5×	3.6	0.39
4		3-*i*Pr	0.0080	3.8×	21×	6.2×	4	0.46
5		3-OCH_3	0.207	1×	7.6×	2.4×	2.7	0.40
6	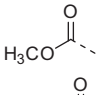	3-*i*Pr	0.0177	7.5×	32.1×	12×	4	0.46
7	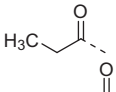	3-*i*Pr	2.2	—	—	—	4.5	0.30
8	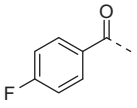	3-*i*Pr	2.2	—	—	—	4.8	0.30

[a] ($JAK1\ K_i/JAK2\ K_i$).
[b] ($JAK3\ K_i/JAK2\ K_i$).
[c] ($TYK2\ K_i/JAK2\ K_i$).
[d] C log *P* values were calculated using MoKa v1.1.0, available from Molecular Discovery Ltd.

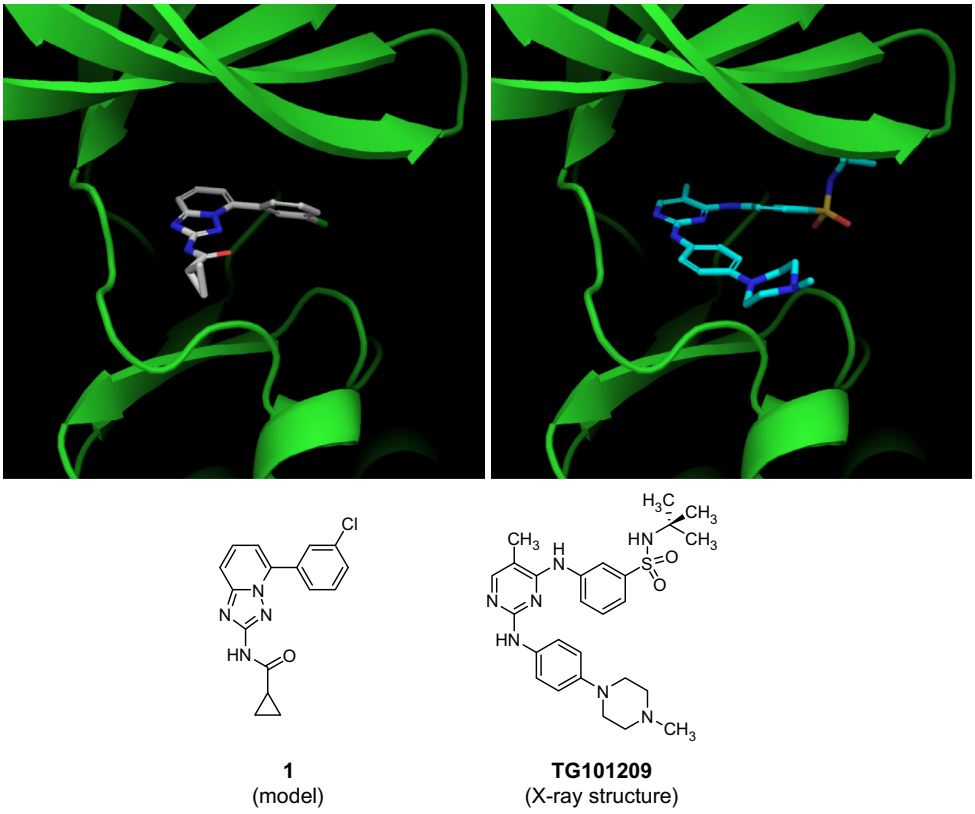

Figure 1. Left: triazolopyridine **1** modeled into X-ray structure of JAK2. Right: X-ray structure of TG101209–JAK2 complex.

Table 2

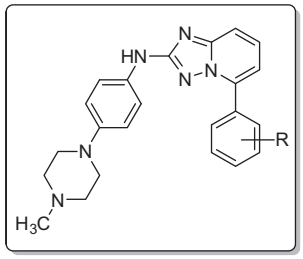

Ex	R	JAK2 K_i (μM)	JAK1 Sel Indx[a]	JAK3 Sel Indx[b]	TYK2 Sel Indx[c]	pSTAT5 SET2 IC_{50} (μM)	Clog*P*[d]	LE
9	4-OCH_3	0.0006	5.4×	12.4×	12.3×	0.0219	5.1	0.41
10	3-SO_2-CH_3	0.0020	11×	22.3×	11×	0.0731	3.9	0.36
11	3-OCH_3	0.0009	12.6×	13.5×	14.2×	0.0536	5.2	0.40
12	4-SO_2-CH_3	0.0003	12.7×	81×	17.4×	0.0329	3.8	0.40

[a] (JAK1 K_i/JAK2 K_i).
[b] (JAK3 K_i/JAK2 K_i).
[c] (TYK2 K_i/JAK2 K_i).
[d] Clog*P* values were calculated using MoKa v1.1.0, available from Molecular Discovery Ltd.

Triazolopyridine **9** has desirable potency and appropriate pharmacokinetic properties in mice (CL_p = 40 mL/min/kg, V_{dss} = 2 L/kg, *F* = 13%) to examine in our pharmacokinetic/pharmacodynamic model, the SET-2 human leukemic cell line derived from a patient with essential thrombocythemia.[14] Mice harboring SET-2 xenograft tumors were treated with a single dose of triazolopyridine **9** at 100 mg/kg. After 1 and 4 h, pSTAT5 and total STAT5 in extracted tumors were measured by MSD electrochemiluminescence detection (Fig. 2). At 1 and 4 h, there was a 75% and 52% reduction in pSTAT5 levels relative to total STAT5, respectively.

With in vivo demonstration of JAK2 inhibition by triazolopyridine **9** in hand, we targeted further improvement of the scaffold for better JAK1 selectivity and pharmacokinetic properties. The phenylpiperazine fragment of triazolopyridine **9** introduced significant binding affinity to JAK2, albeit with an electron-rich aniline. In an attempt to address JAK1 selectivity, a cocrystal structure of triazolopyridine **9** in the JAK2 kinase domain was obtained.[15] In Figure 3, the amino acid residue differences between JAK2 and JAK1 are highlighted. Modification of the phenylpiperazine is expected to impact selectivity since this functional group binds in a

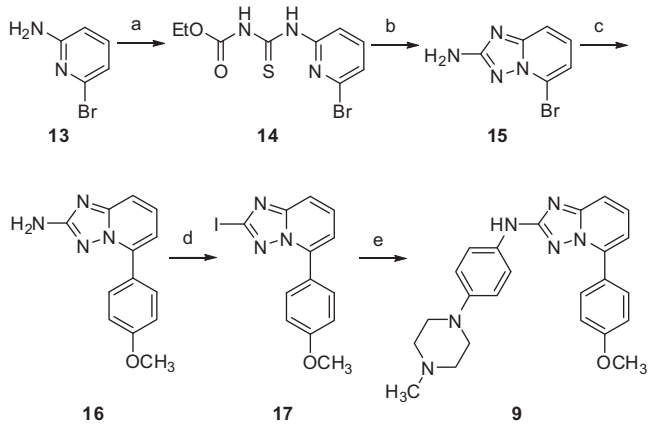

Scheme 1. Synthesis of compound **9**. Reagents and conditions: (a) ethyl isothiocyanatoformate, CH_2Cl_2, 90%; (b) $NH_2OH{\cdot}HCl$, diisopropylethyl amine, 1:1 methanol/ethanol, 70 °C, 80%; (c) $PdCl_2(PPh_3)_2$, Na_2CO_3, 4-methoxyphenylboronic acid, CH_3CN, 120 °C, microwave, 83%; (d) *p*-toluenesolfonic acid, KI, $NaNO_2$, CH_3CN, 71%; (e) 4-(4-methylpiperazin-1-yl)aniline, 2-dicyclohexylphosphino-2′,4′,6′-triisopropylbiphenyl, NaO*t*-Bu, $Pd_2(dba)_3$, $(CH_3)_2NCHO$, 100 °C, 30%.

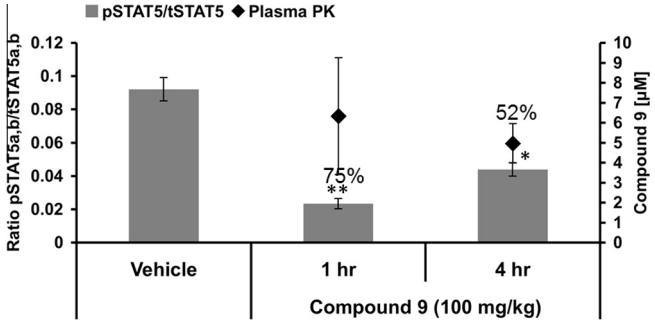

Figure 2. Reduction of pSTAT5α,β in SET2 tumors after dosing of Triazolopyridine **9** (100 mg/kg PO) at 1 and 4 h, student *t*-test $^{*}p$ <0.05, $^{**}p$ <0.001.

region of JAK2 with amino acid residue differences to JAK1 (JAK2 residues 931 on the hinge, 853 above the active site, and 939 which is hydrogen bonded to an observed water).

To improve in vivo metabolic stability and avoid potential reactive metabolites we modified the electron-rich phenylpiperazine.[16] Thus, a series of electron-deficient analogs were prepared that included a variety of substituted pyridine and phenyl isomers (Table 3). 2-Methyl pyridines **18** and **23**, 2-hydroxymethyl pyridine **19** and benzoic acid **24** maintained JAK2 potency with good ligand efficiency. These modifications improved biochemical selectivity against JAK1. Pharmacokinetic evaluation of compound **18** in rats showed high plasma clearance[17] and low bioavailability (CL_p = 42 mL/min/kg, V_{dss} = 1.6 L/kg, F = 3%).

In order to reduce in vivo CL, we subsequently targeted compounds with lower *Clog P* by examining a variety of polar 3-*iso*-propyl phenyl replacements as shown in Table 4. Polar groups such as 3-methylsulfonylphenyl in addition to alkyl pyrazoles were tolerated in terms of inhibition of the JAK2 enzyme; however, evaluation of rat pharmacokinetics revealed that 3-methylsulfonylphenyl **25** (CL_p = 138 mL/min/kg, V_{dss} = 7.2 L/kg, F = 6%) and *N*-ethyl pyrazole **27** (CL_p = 100 mL/min/kg, V_{dss} = 2.4 L/kg, F = 1%) resulted in CL_p that were greater than liver blood flow.[18] The reason for the extremely high plasma clearance was not determined,[19] and similar pharmacokinetic properties for these molecules with a wide lipophilicity range were typically observed. Therefore, further efforts to replace the aminopyridine and to examine an isomeric scaffold were attempted.

An isomeric scaffold was made by repositioning the ring junction nitrogen (Tables 5 and 6). Analogs of the isomeric 8-substituted 2-amino-[1,2,4]triazolo[1,5-*a*]pyridine had similar potency (**24** cf. **29**), and a variety of benzoic acids, benzamides, and pyrazoles[20] were examined. Benzamides **30**–**31** and pyrazoles **32**–**33** maintained biochemical and cellular potency against JAK2. Additionally, the benzamides with low *Clog P* exhibited improved rat in vivo CL_p (Example **31**: in vivo rat CL_p = 10 mL/min/kg, V_{dss} = 0.3 L/kg, F = 15%). Heteroaromatic groups (pyrazole and pyridine) with lipophilic substituents at the C-8 position of the scaffold were also potent inhibitor of JAK2 as shown in Table 6.

Of the examples in Tables 5 and 6, benzoic acid **29** (log*D* (pH 7.4) = 1.01) has the best balance of physical properties. Benzoic acid **29** does not form reactive metabolites (no glutathione adducts upon incubation with liver microsomes and no time dependent inhibition of cytochrome P450s were observed) and exhibits good pharmacokinetic properties in rodents (mouse: CL_p = 15 mL/min/kg, V_{dss} = 0.97 L/kg, F = 81%, PPB = 96.2%; rat: CL_p = 15 mL/min/kg,

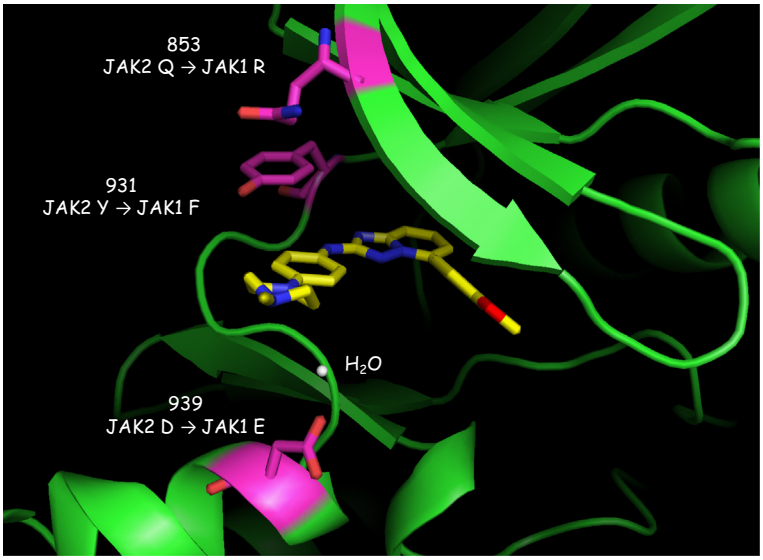

Figure 3. X-ray structure of Triazolopyridine **9** complexed to JAK2 kinase domain. Active site amino acid differences between JAK2 and JAK1 highlighted in magenta.

Table 3

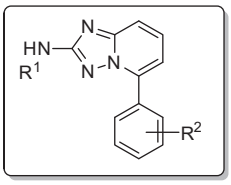

Ex	R^1	R^2	JAK2 K_i (μM)	JAK1 Sel Indx[a]	JAK3 Sel Indx[b]	TYK2 Sel Indx[c]	pSTAT5 SET2 IC_{50} (μM)	*C*log*P*[d]	LE
18	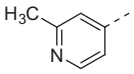	3-*i*-Pr	0.0011	26.3×	18.7×	13.2×	0.190	5.5	0.47
19	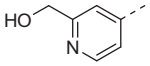	3-*i*-Pr	0.0006	20.8×	27.1×	11.3×	0.117	4.2	0.47
20	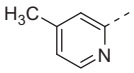	3-*i*-Pr	0.0406	50×	31×	23.6×	1.4	6	0.39
21	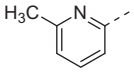	3-*i*-Pr	0.0709	—	—	—	—	6	0.38
22	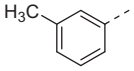	3-*i*-Pr	0.0091	24.1×	17.9×	17.4×	2	6.7	0.42
23	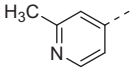	4-OCH_3	0.0050	5.3×	18.3×	7.9×	0.174	4.2	0.46
24	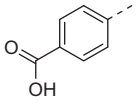	4-OCH_3	0.0016	2.3×	26.2×	5.4×	—	4.9	0.45

[a] (JAK1 K_i/JAK2 K_i).
[b] (JAK3 K_i/JAK2 K_i).
[c] (TYK2 K_i/JAK2 K_i).
[d] *C*log*P* values were calculated using MoKa v1.1.0, available from Molecular Discovery Ltd.

Table 4

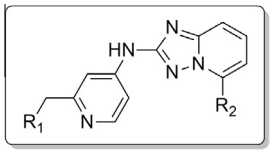

Ex	R^1	R^2	JAK2 K_i (μM)	JAK1 Sel Indx[a]	JAK3 Sel Indx[b]	TYK2 Sel Indx[c]	pSTAT5 SET2 IC_{50} (μM)	*C*log*P*[d]	LE
25	H	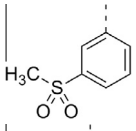	0.0193	9.6×	37×	9×	0.446	2.9	0.39
26	H	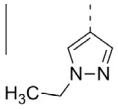	0.0048	8.4×	38×	7.9×	–	3.2	0.48
27	OH	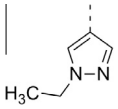	0.003	6×	36×	5×	0.115	1.9	0.47
28	H	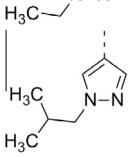	0.002	19.4×	50.9×	11.9×	0.165	4	0.46

[a] (JAK1 K_i/JAK2 K_i).
[b] (JAK3 K_i/JAK2 K_i).
[c] (TYK2 K_i/JAK2 K_i).
[d] *C*log*P* values were calculated using MoKa v1.1.0, available from Molecular Discovery Ltd.

Table 5

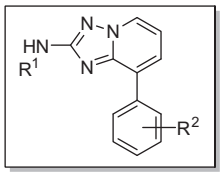

Ex	R^1	R^2	JAK2 K_i (μM)	JAK1 Sel Indx[a]	JAK3 Sel Indx[b]	TYK2 Sel Indx[c]	pSTAT5 SET2 IC_{50} (μM)	*C*log*P*[d]	LE
29	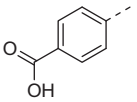	4-OCH_3	0.0017	2.4×	35.2×	7.1×	0.212	4.9	0.45
30	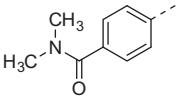	4-SO_2-CH_3	0.0006	8.3×	86.5×	16×	0.117	2.6	0.41
31	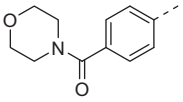	4-SO_2-CH_3	0.0004	11.6×	70×	17.3×	0.0534	2.4	0.38
32	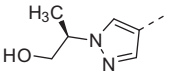	4-OCH_3	0.0014	4.5×	45.9×	11.4×	0.089	3.2	0.45
33	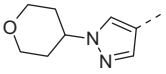	4-OCH_3	0.0007	15.2×	49.5×	21.3×	0.0869	4	0.43

[a] (JAK1 K_i/JAK2 K_i).
[b] (JAK3 K_i/JAK2 K_i).
[c] (TYK2 K_i/JAK2 K_i).
[d] *C*log*P* values were calculated using MoKa v1.1.0, available from Molecular Discovery Ltd.

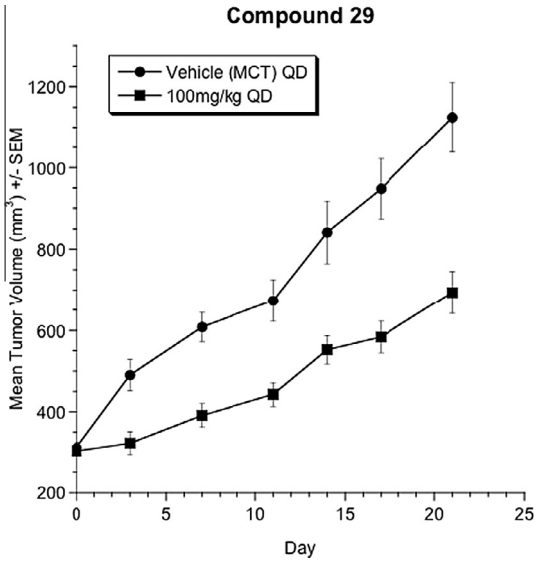

Figure 4. Tumor growth inhibition (38%; *p*-value = 0.0028) in mice (*n* = 10/group) harboring SET-2 acute leukemia xenograft tumors with PO dosing of triazolopyridine **29** QD for 21 days. Percent tumor growth = 100× (mean volume of tumors in animals administered vehicle—mean volume of tumors in animals administered triazolopyridine **29**)/(mean volume of tumors in animals administered vehicle). The *p*-values were calculated using the Dunnett's test using JMP 5.0.

V_{dss} = 0.65 L/kg, *F* = 75%, PPB = 98.3%).[21] Although compound **29** is an acid, the reduced acidity of the 4-aminobenzoic acid moiety may explain the reasonable plasma protein binding, volume of distribution, and absorption. Compound **29** has JAK1 selectivity of 2.4× in our enzyme assays and sufficient JAK2 potency and favorable pharmacokinetic properties to examine in our pharmacodynamic model.

In mice bearing SET-2 xenograft tumors, **29** resulted in significant tumor growth inhibition at 100 mg/kg (daily oral dose) that corresponded to 38% inhibition over 21 days of dosing (Fig. 4).

8-Substituted triazolopyridine **29** is synthesized as shown in Scheme 2. The isomeric triazolopyridine **41** is prepared from 2-amino-3-bromopyridine **39** using similar chemistry as the 5-substituted triazolopyridine **15** (Scheme 1). Amine **41** is converted to carbamate **42** to enhance solubility for the subsequent palladium-mediated cross coupling with 4-methoxyphenyl boronic acid to form biaryl **43** (following an acidic deprotection). Palladium catalyzed amination of amine **43** and methyl 4-iodobenzoate provides **44**. Saponification of the methyl ester affords benzoic acid **29**.

In conclusion, a series of triazolopyridines identified by high-throughput screening were advanced using structure-based design to ligand efficient inhibitors of JAK2 that demonstrate pharmacodynamic response in a human tumor mouse model. During the course of the optimization, we observed poor pharmacokinetic properties for lipophilic and polar compounds with this scaffold. As a result, we introduced an acid moiety to achieve compounds with reasonable pharmacokinetic properties and moderate JAK2 potency and selectivity.

Table 6

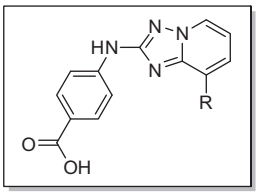

Ex	R	JAK2 K_i (μM)	JAK1 Sel Indx[a]	JAK3 Sel Indx[b]	TYK2 Sel Indx[c]	pSTAT5 SET2 IC_{50} (μM)	*C*log*P*[d]	LE
34	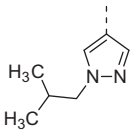	0.0005	6.8×	21×	7.5×	0.156	4.7	0.46
35	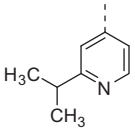	0.0011	16.4×	30.6×	13.1×	0.379	5	0.44
36	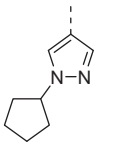	0.0006	8.9×	10×	7.4×	0.0237	4.8	0.44
37	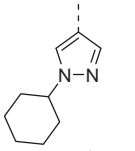	0.0005	8.2×	18.1×	9.6×	0.031	5.2	0.43
38	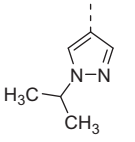	0.0005	7.8×	19.7×	9×	0.151	4.2	0.47

[a] (JAK1 K_i/JAK2 K_i).
[b] (JAK3 K_i/JAK2 K_i).
[c] (TYK2 K_i/JAK2 K_i).
[d] *C*log*P* values were calculated using MoKa v1.1.0, available from Molecular Discovery Ltd.

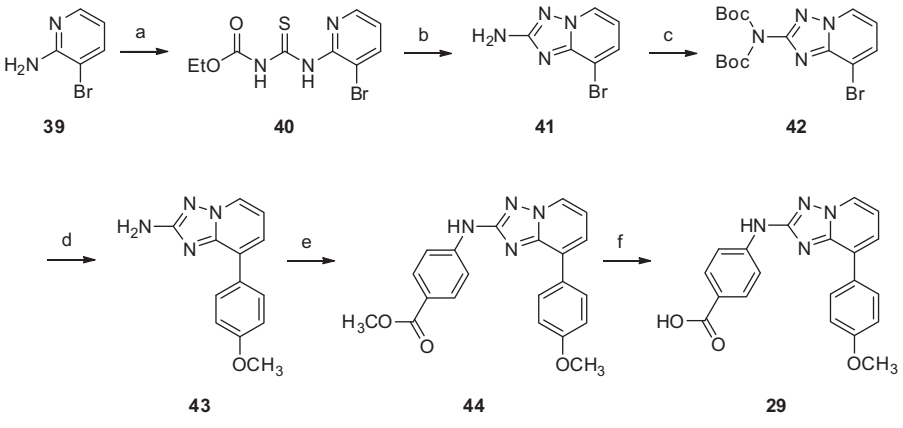

Scheme 2. Synthesis of compound **29**. Reagents and conditions: (a) ethyl isothiocyanatoformate, CH_2Cl_2; (b) $NH_2OH{\cdot}HCl$, diisopropylethyl amine, 1:1 methanol/ethanol, 70 °C, 73% over two-steps; (c) Boc anhydride, *N*,*N*-dimethyl-4-aminopyridine, pyridine, 70%; (d) (i) $Pd(dppf)_2Cl_2$, 4-methoxyphenylboronic acid, K_3PO_4, tetrahydrofuran, 100 °C, (ii) CF_3CO_2H, 79%; (e) $Pd(OAc)_2$, Cs_2CO_3, Xantphos, methyl 4-iodobenzoate, dioxane, 80 °C, 73%; (f) 2 M aqueous NaOH, 85 °C, 75%.

References and notes

1. Yamaoka, K.; Saharinen, P.; Pesu, M.; Holt, V. E. T.; Silvennoinen, O.; O'Shea, J. J. *Genome Biol.* **2004**, *5*, 253.
2. Levine, R. L.; Pardanani, A.; Tefferi, A.; Gilliland, D. G. *Nat. Rev. Cancer* **2007**, *7*, 673.
3. (a) Levine, R. L.; Belisle, C.; Wadleigh, M.; Zahrieh, D.; Lee, S.; Chagnon, P.; Gilliland, D. G.; Busque, L. *Blood* **2006**, *107*, 4139; (b) Baxter, E. J.; Scott, L. M.; Campbell, P. J.; East, C.; Fourouclas, N.; Swanton, S.; Vassiliou, G. S.; Bench, A. J.; Boyd, E. M.; Curtin, N.; Scott, M. A.; Erber, W. N.; Green, A. R. *Lancet* **2005**, *365*, 1054; (c) Kralovics, R.; Passamonti, F.; Buser, A. S.; Teo, S. S.; Tiedt, R.; Passweq, J. R.; Tichelli, A.; Cazzola, M.; Skoda, R. C. *N. Engl. J. Med.* **2005**, *352*, 1779.
4. (a) Kiss, R.; Sayeski, P. P.; Keserú, G. M. *Expert Opin. Ther. Patents* **2010**, *20*, 471. and references cited therein; (b) Wilson, L. J. *Expert Opin. Ther. Patents* **2010**, *20*, 609. and references cited therein; (c) Wrobleski, S. T.; Pitts, W. J. *Annu. Rep. Med. Chem.* **2009**, *44*, 247; (d) Purandare, A. V.; Lorenzi, M. V.; Lombardo, L. J. *Annu. Rep. Med. Chem.* **2010**, *45*, 211.
5. (a) Quintás-Cardama, A.; Verstovsek, S. *Expert Opin. Investig. Drugs* **2011**, *20*, 961. and references cited therein; (b) Lucia, E.; Recchia, A. G.; Gentile, M.; Bossio, S.; Vigna, E.; Mazzone, C.; Madeo, A.; Morabito, L.; Gigliotti, V.; de Stefano, L.; Caruso, N.; Servillo, P.; Franzese, S.; Bisconte, M. G.; Gentile, C.; Morabito, F. *Expert Opin. Investig. Drugs* **2011**, *20*, 41. and references cited therein.
6. Flanagan, M. E.; Blumenkopf, T. A.; Brissette, W. H.; Brown, M. F.; Casavant, J. M.; Shang-Poa, C.; Doty, J. L.; Elliott, E. A.; Fisher, M. B.; Hines, M.; Kent, C.; Kudlacz, E. M.; Lillie, B. M.; Magnuson, K. S.; McCurdy, S. P.; Munchhof, M. J.; Perry, B. D.; Sawyer, P. S.; Strelevitz, T. J.; Subramanyam, C.; Sun, J.; Whipple, D. A.; Changelian, P. S. *J. Med. Chem.* **2010**, *53*, 8468.
7. Verstovsek, S.; Kantarjian, H.; Mesa, R. A.; Pardanani, A. D.; Cortes-Franco, J.; Thomas, D. A.; Estrov, Z.; Fridman, J. S.; Bradley, E. C.; Erickson-Viitanen, S.; Vaddi, K.; Levy, R.; Tefferi, A. *N. Engl. J. Med.* **2010**, *363*, 1117.
8. Contemporaneous to this work, Dugan et al. reported 2-amino-[1,2,4]triazolo[1,5-*a*]pyridines as JAK2 inhibitors. Dugan, B. J.; Gingrich, D. E.; Mesaros, E. F.; Milkiewicz, K. L.; Curry, M. A.; Zulli, A. L.; Dobrzanski, P.; Serdikoff, C.; Jan, M.; Angeles, T. S.; Albom, M. S.; Mason, J. L.; Aimone, L. D.; Meyer, S. L.; Huang, Z.; WellsKnecht, K. J.; Ator, M. A.; Ruggeri, B. A.; Dorsey, B. D. *J. Med. Chem.* **2012**, *55*, 5243.
9. Hopkins, A. L.; Groom, C. R.; Alex, A. *Drug Discovery Today* **2004**, *9*, 430.
10. PDB 4JI9.
11. Pardanani, A.; Hood, J.; Lasho, T.; Levine, R. L.; Martin, M. B.; Noronha, G.; Finke, C.; Mak, C. C.; Mesa, R.; Zhu, H.; Soll, R.; Gilliland, D. G.; Tefferi, A. *Leukemia* **2007**, *27*, 1658.
12. Maestro, version 9.1, Schrodinger, LLC, New York, NY, 2010.
13. Glide, version 5.6, Schrödinger, LLC, New York, NY, 2010 (a) Friesner, R. A.; Banks, J. L.; Murphy, R. B.; Halgren, T. A.; Klicic, J. J.; Mainz, D. T.; Repasky, M. P.; Knoll, E. H.; Shaw, D. E.; Shelley, M.; Perry, J. K.; Francis, P.; Shenkin, P. S. *J. Med. Chem.* **2004**, *47*, 1739; (b) Halgren, T. A.; Murphy, R. B.; Friesner, R. A.; Beard, H. S.; Frye, L. L.; Pollard, W. T.; Banks, J. L. *J. Med. Chem.* **2004**, *47*, 1750; (c) Friesner, R. A.; Murphy, R. B.; Repasky, M. P.; Frye, L. L.; Greenwood, J. R.; Halgren, T. A.; Sanschagrin, P. C.; Mainz, D. T. *J. Med. Chem.* **2006**, *49*, 6177.
14. Uozumi, K.; Otsuka, M.; Ohno, N.; Moriyama, T.; Suzuki, S.; Shimotakahara, S.; Matsumura, I.; Hanada, S.; Arima, T. *Leukemia* **2000**, *14*, 142.
15. PDB 4JIA.
16. (a) Blagg, J. *Annu. Rep. Med. Chem.* **2006**, *41*, 353; (b) Hop, C. E. C. A.; Kalgutkar, A. S.; Soglia, J. R. *Annu. Rep. Med. Chem.* **2006**, *41*, 369; (c) Park, B. K.; Boobis, A.; Clarke, S.; Goldring, C. E.; Jones, D.; Kenna, J. G.; Lambert, C.; Laverty, H. G.; Naisbitt, D. J.; Nelson, S.; Nicoll-Griffith, D. A.; Obach, R. S.; Routledge, P.; Smith, D. A.; Tweedie, D. J.; Vermeulen, N.; Williams, D. P.; Wilson, I. D.; Baillie, T. A. *Nat. Rev. Drug Disc.* **2011**, *10*, 292.
17. Assuming rat liver blood flow = 55 mL/min/kg.
18. Rat liver microsome CLhep: compound **25** = 10 mL/min/kg; compound **27** = 15 mL/min/kg; rat hepatocyte CLhep: compound **25** = 19 mL/min/kg; compound **27** = 37 mL/min/kg).
19. Blood/plasma partition ratios are ~1 for this series.
20. 1-alkyl-4-aminopyrazole as aniline replacements: Zabierek, A. A.; Konrad, K. M.; Haidle, A. M. *Tetrahredron Lett.* **2008**, *49*, 2996.
21. Human liver microsomes CLhep = 6 mL/min/kg; human hepatocyte CLhep = 0.2 mL/min/kg.